SHOCK WAVE SCREENING BY LAYERS OF A VAPOR–GAS–DROP MIXTURE

A. G. Kutushev

UDC 532.529:518.5

Results of mathematical modeling of the effect of screening layers of an inert gas suspension of solid particles upon the interaction of explosive waves with plane obstacles were presented in [1-4]. In the present study, a logical continuation of [1-4], we will describe numerical modeling of the effect of drop suspensions on the reflection of shock wave pulses from a rigid wall. The studies were performed with consideration of possible fractionation and evaporation of drops, as well as condensation of the vapor in the vapor–gas–drop mixture. The numerical computation results are illustrated by characteristic phase parameter profiles at various times in the incident and reflected shock waves, as well as some integral dependences.

1. Fundamental Assumptions and Equations. Assume a two-phase mixture of a three-component (effective) gas (inert gas, vapor, and finely dispersed liquid drops) and large liquid drops. To describe the motion of such a mixture we use the basic assumptions of the mechanics of continuous multiphase dispersed media [5, 6]: the characteristic drop size and distance between drops is much less than the characteristic length of change of macroscopic flow parameters; viscosity and thermal conductivity effects are significant only in interphase interaction processes.

In addition, following [7, 8], we make the following assumptions: the mixture of gas and large drops in its undisturbed state is homogeneous, monodispersed, and in thermodynamic equilibrium; the inert gas and the vapor are ideal calorically perfect gases; the finely dispersed drop component of the gas phase (moisture) and coarse drops are a single-component incompressible liquid; the large drops have spherical form; the velocity and temperature of the moisture coincide with the corresponding parameters of the vapor–gas mixture; the following interphase mass-exchange processes take place between the drops, vapor, and moisture: a) breakup of the large drops in the accompanying gas flow by removal of a thin liquid boundary layer and subsequent instantaneous decay of the removed liquid shroud into a cloud of extremely fine moisture droplets in the gaseous phase; b) evaporation of large drops into the surrounding vapor, or vapor condensation on the surface of large drops; c) equilibrium phase transition between vapor and moisture in the effective gas: moisture and vapor evaporation or vapor condensation on moisture droplets; processes of collision and merger of drops with each other are negligibly small [5].

With consideration of these assumptions the system of differential equations describing one-dimensional unsteady motion of the components of the vapor–gas–drop mixture has the form [8]

$$\frac{\partial \rho_{11}}{\partial t}+\frac{\partial \rho_{11}v_1}{\partial x}=0,\quad \frac{\partial \rho_{12}}{\partial t}+\frac{\partial \rho_{12}v_1}{\partial x}=J_2^v-J_3^v,$$

$$\frac{\partial \rho_{13}}{\partial t}+\frac{\partial \rho_{13}v_1}{\partial x}=J_3^v+J_2^s,\quad \frac{\partial \rho_2}{\partial t}+\frac{\partial \rho_2 v_2}{\partial x}=-J_2^s-J_2^v,\quad \frac{\partial n_2}{\partial t}+\frac{\partial n_2 v_2}{\partial x}=0,$$

$$\frac{\partial \rho_1 v_1}{\partial t}+\frac{\partial \rho_1 v_1^2}{\partial x}+\frac{\partial p}{\partial x}=-F_{12}+\left(J_2^s+J_2^v\right)v_2,$$

$$\frac{\partial \rho_2 v_2}{\partial t}+\frac{\partial \rho_2 v_2^2}{\partial x}=F_{12}-\left(J_2^s+J_2^v\right)v_2,$$

$$\frac{\partial \rho_2 e_2}{\partial t}+\frac{\partial \rho_2 e_2 v_2}{\partial x}=-Q_{2\sigma}-J_2^v e_{2\sigma}-J_2^s e_2,$$

$$\frac{\partial}{\partial t}\left(\rho_1 E_1+\rho_2 E_2\right)+\frac{\partial}{\partial x}\left(\rho_1 E_1 v_1+\rho_2 E_2 v_2\right)+\frac{\partial}{\partial x}\left(p\left(\alpha_1 v_1+\alpha_2 v_2\right)\right)=0,$$

$$\rho_{11}=\rho_{11}^0\alpha_{11},\quad \rho_{12}=\rho_{12}^0\alpha_{12},\quad \rho_{13}=\rho_2^0\alpha_{13},\quad \alpha_{11}=\alpha_{12},\quad \alpha_{11}+\alpha_{13}=\alpha_1,$$

Tyumen. Translated from Prikladnaya Mekhanika i Tekhnicheskaya Fizika, No. 4, pp. 38-46, July-August, 1993. Original article submitted June 16, 1992.

0021-8944/93/3404-0486$12.50 © 1994 Plenum Publishing Corporation

$$E_1 = e_1 + 0{,}5v_1^2, \quad E_2 = e_2 + 0{,}5v_2^2, \quad \alpha_2 = \frac{\pi d_2^2 n_2}{6},$$
$$\rho_1 = \rho_{11} + \rho_{12} + \rho_{13}, \quad \rho_1 = \rho_1^0\alpha_1, \quad \rho_2 = \rho_2^0\alpha_2, \quad \alpha_1 + \alpha_2 = 1. \tag{1.1}$$

Equation (1.1) expresses the laws of conservation of mass of effective gas components (inert gas, vapor, and finely dispersed moisture), conservation of mass and number of large drops, conservation of momentum of the effective gas and large drops, conservation of total energy of the entire mixture as a whole, and the equation of heat influx into the dispersed phase. The subscripts 11, 12, 13 refer to the inert gas, vapor, and moisture, while 1, 2 refer to parameters of the carrier gas and dispersed condensed phase; the symbols ρ, ρ^0, α, v, e, E denote mean and true density, volume content, mass velocity, specific internal and total energy; d_2 and n_2 are the diameter and number of large drops per unit volume of the mixture; F_{12} is the intensity of the force interaction between carrier and dispersed phase; $Q_{2\sigma}$ is the intensity of the heat input to the interphase surface (σ-phase) from the dispersed phase; p is the vapor–gas mixture pressure; $e_{2\sigma}$ is the intensity of the large drop surface layer removal; J_2^S is the intensity of the surface layer removal of large drops; J_2^V is the intensity of large drop evaporation or vapor condensation onto large drops; J_3^V is the intensity of the equilibrium phase transition between vapor and moisture.

The equations of state for the inert gas, vapor, moisture, and large drops appear as follows [5, 6]:

$$p_{11} = \rho_{11}^0 R_{11} T_1, \quad e_{11} = c_{11} T_1,$$
$$p_{12} = \rho_{12}^0 R_{12} T_1, \quad e_{12} = c_{12}(T_1 - T_0) + e_{12}^0, \quad \rho_2^0 = \text{const},$$
$$e_{13} = c_2(T_1 - T_0) + e_2^0, \quad e_2 = c_2(T_2 - T_0) + e_2^0,$$
$$e_{2\sigma} = c_2(T_\sigma - T_0) + e_2^0,$$
$$e_2^0 - e_{12}^0 = (c_2 - c_{12}) T_0 - \left[(c_2 - \gamma_{12}c_{12}) T_s(p_0) + \frac{p_0}{\rho_2^0} + l(p_0)\right]$$
$$\left(R_{11},\ R_{12},\ c_{11},\ c_{12},\ c_2,\ e_{12}^0,\ e_2^0,\ l(p_0) \equiv \text{const}\right). \tag{1.2}$$

Here p_{1k}, e_{1k}, R_{1k}, c_{1k}, γ_{1k} are the partial pressure, specific internal energy, gas constant, specific heat at constant volume and adiabatic index of component k of the three-component effective gas (k = 1, 2, 3); T_i, T_σ, T_0 are the temperature of phase i, the interphase surface, and the initial temperature; e_{12}^0 and e_2^0 are constants satisfying normalization conditions; p_0 is the initial pressure of the gas mixture at $T_1 = T_0$; T_S is the vapor saturation temperature; and $\ell(p_0)$ is the specific heat of vapor formation.

In accordance with Dalton's law, as well as the condition of additiveness of internal energy of the gas mixture over masses of the components, the equations of state of the effective gas have the form

$$p = \rho_1^0 R_1 T_1 \quad \left(R_1 = x_{11}R_{11} + x_{12}R_{12};\ \ x_{11} = \frac{\rho_{11}}{\rho_1};\ \ x_{12} = \frac{\rho_{12}}{\rho_1}\right),$$
$$e_1 = c_1(T_1 - T_0) + e_1^0 \left(c_1 = x_{11}c_{11} + x_{12}c_{12} + x_{13}c_2;\ \ x_{13} = \frac{\rho_{13}}{\rho_1}\right), \tag{1.3}$$
$$e_1^0 = x_{11}e_{11}^0 + x_{12}e_{12}^0 + x_{13}e_2^0.$$

The intensities of the force interaction and contact heat exchange between the carrier gas flow and the large drops are specified by the expressions [6]

$$F_{12} = \frac{0{,}75\alpha_2 C_d \rho_1^0 |v_1 - v_2|(v_1 - v_2)}{d_2}, \quad Q_{i\sigma} = \frac{6\alpha_2 \varepsilon \mathrm{Nu}_i \lambda_i (T_i - T_\sigma)}{d_2^2},$$
$$C_d = \begin{cases} 27\,\mathrm{Re}_{12}^{-0.84}, & 0 < \mathrm{Re}_{12} \leqslant 80, \\ 0{,}27\,\mathrm{Re}_{12}^{0.217}, & 80 < \mathrm{Re}_{12} \leqslant 10^4, \\ 2, & \mathrm{Re}_{12} > 10^4, \end{cases}$$
$$\mathrm{Nu}_1 = 2 + 0{,}6\,\mathrm{Re}_{12}^{0.5}\,\mathrm{Pr}_1^{0.33}, \ \mathrm{Nu}_2 = 10, \ \mathrm{Pr}_1 = \frac{c_{p1}\mu_1}{\lambda_1}, \tag{1.4}$$
$$\mathrm{Re}_{12} = \frac{\rho_1^0 |v_1 - v_2| d_2}{\mu_1}, \quad \mu_1 = x_{11}\mu_{11} + x_{12}\mu_{12} + x_{13}\mu_2,$$
$$c_{p1} = x_{11}c_{p11} + x_{12}c_{p12} + x_{13}c_2, \quad \lambda_1 = x_{11}\lambda_{11} + x_{12}\lambda_{12} + x_{13}\lambda_2.$$

where C_d is the drop aerodynamic resistance coefficient; Re_{12} is the Reynolds number for the relative motion of gaseous and dispersed phases; Nu_i, λ_i, μ_i are the Nusselt number, thermal conductivity, and dynamic viscosity of phase i (i = 1, 2); λ_{1k}, μ_{1k}, c_{p1k} are coefficients of thermal conductivity, dynamic viscosity, and specific heat at constant pressure for phase k of the gaseous phase (k = 1, 2); and Pr_1 is the Prandtl number.

The parameter ε, appearing in Eq. (1.4) for $Q_{i\sigma}$ takes on values of 0 and 1 for the cases of presence ($We \geqslant We_*$) and absence ($We < We_*$) of drop breakup in the gas flow. Here We and We_* are the Weber number and critical Weber number value

$$We = \frac{\rho_1^0 (v_1 - v_2)^2 d_2}{\sigma_2} \quad (\sigma_2 = \text{const}) \tag{1.5}$$

(σ_2 is the liquid surface tension coefficient at the boundary with the gas).

The intensity of interphase mass exchange by the large drop surface layer removal mechanism can be specified by an expression of the type [6, 9, 10]

$$J_2^s = (1-\varepsilon) k_J \left(\frac{\rho_1^0}{\rho_2^0}\right)^{0,33} \left(\frac{\nu_1}{\nu_2}\right)^{0,16} \nu_2^{0,5} |v_1 - v_2|^{0,5} \left(\frac{d_2}{2}\right)^{1,5} \rho_2^0 n_2 \quad (k_J \simeq 12), \tag{1.6}$$

where $\nu_i = \mu_i/\rho_i^0$ is the kinematic viscosity of phase i (i = 1, 2). Then, according to [11],

$$We_* = k_s \, Re_{12}^{0,5} \quad (k_s \simeq 1). \tag{1.7}$$

In accordance with the hypothesis of quasi-equilibrium of the flow of the liquid evaporation and vapor condensation processes [$T_\sigma = T_S(p_{12})$] the intensity of phase conversion J_2^V can be defined from the thermal balance equation on the interphase boundary [5]:

$$J_2^v = \frac{\varepsilon (Q_{1\sigma} + Q_{2\sigma})}{l}. \tag{1.8}$$

To find the dependence $T_S(p_{12})$ we make use of the Clapeyron–Clausius equation [12]

$$\frac{dT_s}{dp_{12}} = \frac{T_s (1 - \rho_{12}^0/\rho_2^0)}{\rho_{12}^0 l}. \tag{1.9}$$

In analogy to [7, 8] the intensity of mass exchange in the gas phase between vapor and moisture can be found from the equation of heat influx for the effective gas written on the saturation line $T_1 = T_S$:

$$J_3^v = \left(\frac{\partial e_1}{\partial x_{13}}\right)^{-1} \left\{ p \frac{\partial}{\partial x} (\alpha_1 v_1 + \alpha_2 v_2) + \left[p \left(\frac{1}{\rho_2^0} - \frac{1}{\rho_1^0}\right) - \left(x_{11} \frac{\partial e_1}{\partial x_{11}} + x_{13} \frac{\partial e_1}{\partial x_{13}}\right) - \right.\right.$$

$$\left.\left. - \frac{(v_1 - v_2)^2}{2} \right] (J_2^v + J_2^s) + \left(\frac{\partial e_1}{\partial x_{13}} - e_2 + e_1\right) J_2^s - (i_{12s} - i_1) J_2^v - (v_1 - v_2) F_{12} + Q_{1\sigma} + \rho_1 \frac{\partial e_1}{\partial T_s} \frac{dT_s}{dp_{12}} \frac{d_1 p_{12}}{dt} \right\}. \tag{1.10}$$

The derivative $d_1 p_{12}/dt$ is determined from the equation of state of the vapor.

2. Formation of the Problem and Some Results of the Numerical Study. At the initial moment t = 0 a plane shock wave with triangular gas mass velocity profile moves from the region ($0 \leqslant x \leqslant x_f$) of the two-component gas mixture (inert gas and vapor) in the direction of a solid rigid wall ($x = x_w$) screened by a layer of homogeneous monodispersed vapor–gas–drop mixture ($x_f < x < x_w$). Our task is to study the evolution of the shock wave in the screening layer.

Initial conditions for this problem are formulated as in [1]:

$$v_1 = v_{1f} \frac{x}{x_f}, \quad \alpha_1 = \alpha_{11} = \alpha_{12} = 1, \quad \alpha_2 = \alpha_{13} = 0,$$

$$\rho_1^0 = \rho_{1f}^0 (\varphi(x))^{2/(\gamma_1 - 1)}, \quad p = p_f (\varphi(x))^{2\gamma_1/(\gamma_1 - 1)}, \quad T_1 = \frac{p}{(\gamma_1 - 1) c_1 \rho_1^0},$$

$$\rho_{12}^0 = \rho_1^0 \frac{(\gamma_1 - 1) c_1 - (\gamma_{11} - 1) c_{11}}{(\gamma_{12} - 1) c_{12} - (\gamma_{11} - 1) c_{11}}, \quad \rho_{11}^0 = \rho_1 - \rho_{12}^0$$

$$\left(\varphi(x) = 1 - \frac{(\gamma_1 - 1)}{2} \frac{v_{1f}}{a_{1f}} \left(1 - \frac{x}{x_f}\right), \quad a_{1f}^2 = \gamma_1 \frac{p_f}{\rho_{1f}^0}, \quad 0 \leqslant x \leqslant x_f\right),$$

$$v_1 = v_2 = 0, \quad \alpha_1 = \alpha_{11} = \alpha_{12} = \alpha_{10}, \quad \alpha_2 = \alpha_{20}, \quad \alpha_{13} = 0,$$

$$\rho_1^0 = \rho_{10}^0,\ \rho_{12}^0 = \rho_{120}^0,\ \rho_{11}^0 = \rho_{10}^0 - \rho_{120}^0,\ \rho_2 = \rho_2^0\alpha_{20},$$
$$p = p_{110} + p_{120} = p_0,\quad T_1 = T_2 = T_s(p_{120}) = T_0,\quad d_2 = d_{20},\quad n_2 = n_{20} \qquad (2.1)$$
$$(x_f < x < x_w).$$

Here γ_1 is the adiabatic index of the vapor–gas mixture; the gas parameters ahead of and behind the shock wave are related by the Rankine–Hugoniot relationships

$$\frac{\rho_{1f}^0}{\rho_{10}^0} = \frac{(\gamma_1+1)M_0^2}{2+(\gamma_1-1)M_0^2},\ \frac{v_{1f}}{a_{10}} = \frac{2}{(\gamma_1+1)}\left(M_0 - \frac{1}{M_0}\right),\ \frac{p_f}{p_0} = 1 + \frac{2\gamma_1}{\gamma_1+1}(M_0^2-1), \qquad (2.2)$$

where M_0 is the Mach number of the incident shock wave.

On the left boundary of the calculation region (x = 0) we impose the condition of free passage of the gas phase [13-15]:

$$v_1(0_-,\ t) = v_1(0_+,\ t). \qquad (2.3)$$

No boundary condition was specified for drops at x = 0 in view of their absence during the entire motion process. On the right side of the calculation region ($x = x_w$), the wall, we specify nonpassage of the gas and free passage of drops, modeling their outflow upon inelastic interaction with the obstacle [13-15]:

$$v_1(x_w,\ t) = 0,\quad v_2(x_{w-},\ t) = v_2(x_{w+},\ t). \qquad (2.4)$$

The problem thus formulated is a mixed problem for a system of quasilinear differential equations in partial derivatives (1.1)-(1.10) with initial (2.1), (2.2) and boundary conditions (2.3), (2.4). A numerical solution was obtained by the large particle method [13] with an algorithm for localization of the drop cloud boundary [14, 15]. The calculations were performed with an ES-1066 computer.

The calculations were performed for a vapor–gas–drop mixture of air, water vapor, and water drops. The following values were used for the thermodynamic parameters of the phases and their components: T_0 = 293 K, $p_0 = 1.01\cdot10^{-5}$ N/m^2, $\rho_{10}^0 = 1.21$ kg/m^3, $\gamma_{10} = 1.4$, $c_{10} = 716$ m^2/(sec^2·deg), $\mu_1 = 1.85\cdot10^{-5}$ kg/(m·sec), $\lambda_1 = 2.5\cdot10^{-2}$ kg·m/(sec^3·deg), $a_{10} = 341$ m/sec, $p_{110} = 0.976\cdot10^5$ N/m^2, $\rho_{110}^0 = 1.19$ kg/m^3, $\gamma_{11} = 1.39$, $c_{11} = 704.5$ m^2/(sec^2·deg), $\mu_{11} = 1.85\cdot10^{-5}$ kg/(m·sec), $\lambda_{11} = 2.5\cdot10^{-2}$ kg·m/(sec^3·deg), $p_{120} = 2.4\cdot10^3$ N/m^2, $\rho_{120}^0 = 1.89\cdot10^{-2}$ kg/m^3, $\gamma_{12} = 1.3$, $c_{12} = 1442$ m^2/(sec^2·deg), $\mu_{12} = 8.85\cdot10^{-6}$ kg/(m·sec), $\lambda_{12} = 1.88\cdot10^{-2}$ kg·m/(sec^3·deg), $\rho_2^0 = 998$ kg/m^3, $c_2 = 4180$ m^2/(sec^2·deg), $\mu_2 = 10^{-3}$ kg/(m·sec), $\lambda_2 = 0.6$ kg·m/(sec^3·deg), $\sigma_2 = 0.073$ N/m.

Shock wave intensity was specified at M_0 = 5.1 and 7. Shock wave lengths at the initial moment were taken as ℓ_b = 0.048, 0.22, and 0.4 m, with drop gas suspension screening layer extending ℓ_s = 0.05, 0.25, and 1 m. The initial relative mass content $m_{20} = \rho_{20}/\rho_{10}$ and initial drop diameter d_{20} were varied over the ranges $0 \leqslant m_{20} \leqslant 4$ and $0 \leqslant d_{20} \leqslant 1200$ μ.

Figures 1, 2 show characteristic pressure and gas temperature profiles behind a shock wave (M_0 = 7, ℓ_b = 0.4 m) penetrating into a layer of vapor–gas–drop mixture (ℓ_s = 1 m, m_{20} = 0.82, d_{20} = 600 μ), located in front of a rigid wall ($x_w = \ell_b + \ell_s$ = 1.4 m). The solid and dashed lines indicate solutions corresponding to consideration (J_2^s, J_2^v, $J_3^v \neq 0$) and nonconsideration ($J_2^s = J_2^v = J_3^v \equiv 0$) of interphase mass exchange processes at times t_i = 0.18i msec (i = 0-3, curves 0-3).

As is evident from Fig. 1, as it propagates through the screening layer the shock wave with initially triangular pressure profile is intensely attenuated. The attenuation is produced by both an overtaking rarefaction wave, as well as dissipative interphase interaction processes (friction and heat-mass exchange). Detailed evaluation of the effects of force and thermal phase interactions on the evolution of the passing shock wave in a screening layer of gas suspension was carried out in [1-4]. Thus it will be desirable to note only the effect of interphase mass exchange processes on the dynamics of shock wave propagation in the cloud of vapor–gas–drop mixture.

Calculations show that for the examples of motion considered here, among the processes of interphase mass exchange realized in transient shock waves in vapor–gas–drop media the most intense, and therefore controlling, is the process of drop destruction by the gas flow. The intensity of drop breakup J_2^s is an order of magnitude greater than the intensity of drop evaporation J_2^v. Moreover, behind transient shock waves with a "triangular" gas mass velocity profile over practically the entire region of disturbed phase motion drop destruction occurs

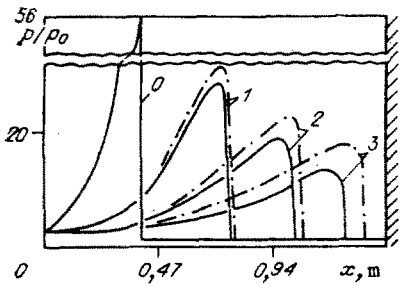

Fig. 1

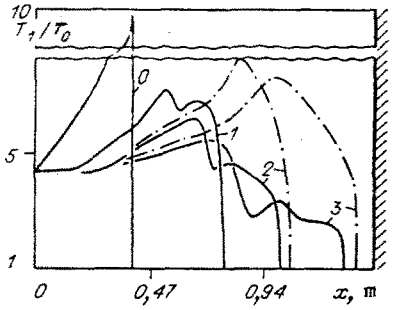

Fig. 2

by surface layer removal ($We > We_*$). As a rule, evaporation of large drops occurs only in a narrow region of two-phase motion up the flow from the shock wave front, where $v_2 \approx v_1$.

It is evident from Figs. 1, 2 that presence of drop breakup and evaporation encourage greater attention of the passing shock wave as compared to the case of absence of mass exchange between the mixture phases (compare the solutions shown by solid and dash-dot lines). Consideration of interphase mass exchange processes leads to a marked decrease in gas pressure and temperature, as well as reduced density of the gas suspension drops. Thus, it has been shown that due to realization of drop breakup and evaporation, significant losses in internal energy of the gas flow occur, causing more intense attenuation of the passing shock wave (as compared to the case of shock wave attenuation in an identical but inert gas suspension of solid particles).

Upon subsequent interaction of the incident shock wave with the rigid wall ($x = x_w$) a transient reflected shock wave is formed, behind the front of which drop breakup is also observed, reducing the gas temperature and pressure in the vicinity of the obstacle, due to velocity nonequilibrium of the phases. To illustrate the effect of interphase mass exchange on the parameters of the shock wave reflected from the rigid wall we turn to Fig. 3, which shows calculated pressure (a) and temperature (b) profiles corresponding to Figs. 1, 2 for the gaseous phase in a vapor–gas–drop mixture at times 0.72 and 0.9 msec (curves 1, 2). Solid and dash-dot lines show solutions obtained with and without consideration of interphase mass exchange.

The numerical calculation results shown in Fig. 3 correspond to situations where the condition $We > We_*$ is satisfied over practically the entire disturbed flow region behind the wave reflected from the wall, i.e., interphase mass exchange is accomplished by the mechanism of removal of the drop surface layer by the gas flow and subsequent instantaneous evaporation of the removed microdroplets. As is evident from Fig. 3, drop breakup in the shock wave reflected from the wall intensely encourages reduction in gas pressure and temperature.

It is interesting to consider the effect of the parameters of a drop suspension screening layer located directly between the incident shock wave front and the obstacle upon the maximum (peak) pressure behind the shock wave reflected from the wall. As an example, Fig. 4 shows integral dependences of maximum pressure p_m/p_0 at the barrier upon initial relative mass content of drops in the mixture m_{20} for various initial liquid drop sizes. Curves 0 and 5 correspond to limiting equilibrium ($d_{20} \to 0$) and frozen ($d_{20} \to \infty$) solutions, curves 1 and 3, to solutions obtained with consideration of interphase mass exchange, and 2 and 4, to solutions obtained without consideration of drop breakup and evaporation or vapor condensation. For curves 1 and 2 the initial drop size $d_{20} = 600$ μ, for 3 and 4, $d_{20} = 1200$ μ. Also $\ell_s = 0.25$ m, $M_0 = 5.1$, $\ell_b = 0.22$ m, left boundary of drop cloud located at $x_* = 0.26$ m, and wall at $x_w = 0.48$ m.

It is evident from the numerical solutions shown in Fig. 4 that with increase in initial relative mass content of the drop suspension in a screening layer with fixed initial drop size there is a decrease in peak pressure on the barrier behind the reflected shock wave. The latter is valid for both consideration and neglect [1] if interphase mass exchange processes.

Other conditions being equal, consideration of interphase mass exchange, primarily drop breakup, leads to significantly greater shock wave attenuation as compared to nonconsideration of interphase mass exchange. In particular, comparison of curves 1 and 2 ($d_{20} = 600$ μ) as well as curves 3 and 4 ($d_{20} = 1200$ μ) in Fig. 4 shows that at $m_{20} = 4$ those solutions can differ by a factor of two. As was noted above, more intense attenuation of shock waves in

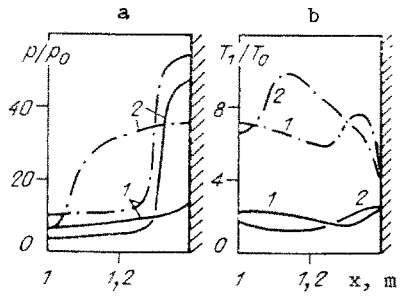

Fig. 3

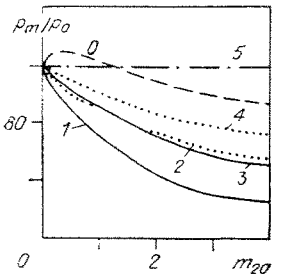

Fig. 4

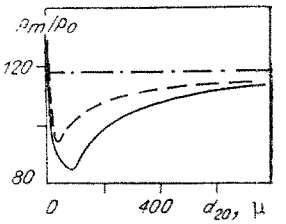

Fig. 5

layers with disintegrating and evaporating drops as comapred to identical layers bearing solid particles is caused by stripping of the surface layers of large drops with subsequent evaporation of the moisture thus removed. It is also clear that with increase in m_{20} in the mixture the intensity of phase conversion increases ($J_2^S \sim m_{20}$), and thus gas thermal losses increase.

Analysis of the numerical solutions presented in Fig. 4 indicates that in drop curtains with fixed m_{20} the peak pressure at the barrier depends nonmonotonically upon initial drop size. This is illustrated more clearly and in greater detail by Fig. 5, which shows calculated dependences of maximum pressure on the wall upon initial drop size at $m_{20} = 0.5$. Calculations were performed for a screening layer of drop suspension with $\ell_b = 0.05$ m, $\ell_s = 0.05$ m, $M_0 = 5.1$. The solid and dashed lines correspond to consideration and neglect of interphase mass exchange phenomena, the dash-dot line to the limiting frozen solution as $d_{20} \to \infty$. It is evident from Fig. 5 that in the cases of either consideration or neglect of drop breakup and evaporation there are characteristic minima in the functions $p_m(d_{20})$. These minima correspond to the greatest attenuation of the shock waves by the drop curtains for a fixed m_{20}. For interphase mass exchange processes the minimum is less than for an identical suspension of solid inert particles. Moreover, the value of d_{20} at which the p_m minimum occurs when phase transitions are present is higher than d_{20} in their absence.

A qualitative acoustical explanation of the minimum in $p_m(d_{20})$ was presented in [3], and it was noted that the minimum occurs at $\tau_v/\tau_b \sim 1$ (where τ_v and τ_b are the characteristic time of dynamic phase interaction and the duration of the shock wave pulse). Since $\tau_v \sim \tau_v^0/((1 + m_{20})f(M_0))$ [$f(M_0) > 0$ is a positive function and τ_v^0 is the characteristic time for equalization of the velocity of an isolated particle], one can expect in the case $\tau_b = \text{const}$ that with increase in shock wave intensity M_0 and relative particle mass content m_{20} the minimum in $p_m(d_{20})$ will shift in the direction of lower d_{20}. The calculations performed confirm these concepts.

In conclusion, we will note that it has been shown by the numerical studies performed that, other conditions being equal, use of drop curtains to extinguish shock waves is more efficient than use of screening layers of inert gas suspensions of solid particles.

The author thanks U. A. Nazarov for his assistance in performing the calculations.

LITERATURE CITED

1. A. I. Ivandaev and A. G. Kutushev, "Effect of gas suspension screening layers on shock wave reflection," Prikl. Mekh. Tekh. Fiz., No. 1 (1985).
2. B. S. Kruglikov and A. G. Kutushev, "Attenuation of air shock waves by layers of dusty gas and lattices," Prikl. Mekh. Tekh. Fiz., No. 1 (1988).
3. R. I. Nigmatulin, A. G. Kutushev, and N. A. Gumerov, "Some features of the effect of dust particles on interaction of shock waves in gas suspensions with boundaries," in: Chemical Physics of Combustion and Explosion Processes. Problems of Combustion and Explosion. Materials of the 9th All-Union Symposium on Combustion and Explosion, Chernogolovka (1989).
4. A. G. Kutushev, "Screening properties of homogeneous and inhomogeneous layers of mono- and polydispersed gas suspensions," in: Dynamics of Continuous Media, Collected Scientific Studies, Russian Academy of Science, Siberian Branch, Hydrodynamics Institute, No. 100 (1991).
5. R. I. Nigmatulin, Dynamics of Multiphase Media [in Russian], Part 1, Nauka, Moscow (1987).
6. A. I. Ivandaev, A. G. Kutushev, and R. I. Nigmatulin, "Gas dynamics of multiphase media. Shock and detonation waves in gas suspensions," in: Achievements in Science. Liquid and Gas Mechanics [in Russian], Vol. 16, VINITI, Moscow (1981).

7. S. V. Tarakanov, I. Yu. Pavlov, O. M. Todes, and A. D. Gol'tsiker, "Analysis of formation of a relaxation shock wave in an air suspension of chemically inert liquid particles," Vzryvn. Del., No. 80/37 (1978).
8. T. R. Amanbaev and A. I. Ivandaev, "Shock wave structure in two-phase mixtures of gas with liquid drops," Prikl. Mekh. Tekh. Fiz., No. 2 (1988).
9. O. G. Engel, "Fragmentation of water drops in the zone behind an air shock," J. Res. Nat. Bur. Stand., 60, No. 3 (1958).
10. A. A. Ranger and J. A. Nicholls, "Aerodynamic scattering of liquid drops," AIAA J., 7, No. 2 (1969).
11. A. A. Borisov, B. E. Gel'fand, M. S. Natanzon, and O. M. Kossov, "Drop fragmentation regimes and criteria for their existence," Inzh. Fiz. Zh., 40, No. 1 (1981).
12. I. P. Bazarov, Thermodynamics [in Russian], Vysshaya Shkola, Moscow (1983).
13. O. M. Belotserkovskii and Yu. M. Davydov, The Coarse Particle Method in Gas Dynamics [in Russian], Nauka, Moscow (1982).
14. A. A. Gubaidullin, A. I. Ivandaev, and R. I. Nigmatulin, "A modified 'coarse particle' method for calculation of nonsteady wave processes in multiphase dispersed media," Zh. Vychisl. Mat. Mat. Fiz., 17, No. 6 (1977).
15. A. I. Ivandaev and A. G. Kutushev, "Numerical study of nonsteady wave flows of gas suspensions with detection of boundaries of two-phase regions and contact discontinuities in the carrier gas," ChMMSS, 14, No. 6 (1983).

CHANGE IN THE SHAPE AND CHARACTERISTICS OF A BURNING BODY IN HYPERSONIC FLOW

S. Yu. Menzhinskii and N. N. Pilyugin

UDC 536.46

The investigation of hypersonic flow around burning models is of interest in order to develop a mathematical theory of internal ballistics, to understand the combustion of solid fuel as it exists from an engine nozzle, to simulate the physical processes in meteoric phenomena [1], and to study features of the combustion and detonation of explosive gas mixtures. By now, stationary combustion of carbon or materials with carbon thermal protective coatings have been rather completely studied [2]. At the same time, no such analysis exists for material with a complex arbitrary chemical composition, and it is necessary to use mainly empirical data. One problem which has not been investigated is how the surface of a body burns in hypersonic motion and how its aerodynamic characteristics change. Results from a ballistic range of experiments have been presented [1] on mass removal from rapidly burning models of made of pyrotechnic materials and on the hypersonic flow around them.

Here we find the shape change when spherical or parabolic bodies are burned, and we also find the resistance and mass after the hypersonic motion on a ballistic track under the same conditions as in [1]. We calculated how the radius of curvature and the lateral area, which determines the luminosity of the burning models, changes with time.

1. Basic Concepts and Assumptions. Today there are a large number of different mechanisms which explain the combustion of solid fuels of a given composition [3]. A simplified combustion model for the solid surface of a pyrotechnic powder is as follows. It is assumed that the chemical reaction is initiated by instantaneous ignition of the model in a barrel [4] and then proceeds by a very simple method: oxygenated fuel → gaseous reaction products. All heat going from the reaction zone to the solid phase is sufficient to maintain continuous combustion of the thermal flow. It is assumed [3, 4] that the temperature of the burning surface is constant, that the combustion is one-dimensional and goes layer by layer, and that the material is gasified in a narrow zone at the surface. The gas phase is treated as a quasi-stationary phase which instantaneously adds to the thermal state of the surface layer.

According to current ideas, the flow of combustion products which move along the surface has a strong effect on the heat and mass transfer. Turbulization of the boundary layer intensifies the transfer processes and also increases convective heat transfer, which increases

Moscow. Translated from Prikladnaya Mekhanika i Tekhnicheskaya Fizika, No. 4, pp. 46-55, July-August, 1993. Original article submitted April 8, 1992; revision submitted July 27, 1992.

 0021-8944/93/3404-0492$12.50 © 1994 Plenum Publishing Corporation